Non-resonant and non-enhanced Raman Correlation Spectroscopy

A. Barbara, F. Dubois, P. Quemerais, L. Eng

Non-resonant and non-enhanced Raman Correlation Spectroscopy

A. Barbara,[1,2,*] **F. Dubois,**[1] **P. Quémerais,**[1] **and L. Eng**[2]

[1]*Institut Néel, CNRS et Université Joseph Fourier, BP 166, F-38042 Grenoble Cedex 9, France*
[2]*Institut für Angewandte Photophysik, Technische Universität Dresden, 01062 Dresden, Germany*

**aude.barbara@grenoble.cnrs.fr*

Abstract: We present the first non-resonant and non-enhanced Raman correlation spectroscopy experiments. They are conducted on a confocal microscope combined with a Raman spectrometer. The thermal fluctuations of the Raman intensities scattered by dispersions of polystyrene particles of sub-micrometric diameters are measured and analysed by deriving the autocorrelation functions (ACFs) of the intensities. We show that for particles of diameter down to 200 nm, RCS measurements are successfully obtained in spite of the absence of any source of amplification of the Raman signal. For particles of diameter ranging from 200 to 750 nm, the ACFs present a time-decay behaviour in accordance with the model of free Brownian particles. For particles of 1000 nm in diameter, the AFCs present a different behaviour with a much smaller characteristic time. This results from the dynamics of a single-Brownian particle trapped in the confocal volume by the optical forces of the focus spot.

OCIS codes: (120.0120) Instrumentation, measurement, and metrology; (120.6200) Spectrometers and spectroscopic instrumentation; (270.5290) Photon statistics.

References and links

1. L. Gouÿ, "Notes sur le mouvement Brownien," J. de Phys. **7**(2), 561-563 (1888).
2. A. Einstein, "On the movement of small particles suspended in stationary liquids required by the molecular-kinetic theory of heat," Ann. d. Phys. **17**, 549-560 (1905).
3. L. Bachelier, "Théorie de la spéculation," Ann. sci. de l'ENS **17**(3), 21-86 (1900).
4. S. Chandrasekhar, "Stochastic problems in physics and astronomy," Rev. Mod. Phys. **15**(1), 1-89 (1943).
5. H. Z. Cummins, N. Knable and Y. Yeh, "Observation of diffusion broadening of Rayleigh light," Phys. Rev. Lett. **12**(6), 150-153 (1964).
6. B. J. Berne and R. Pecora, *Dynamic Light Scattering with Applications to Chemistry, Biology, and Physics* (Ed. Wiley & Sons, 1975).
7. N. Pusey and B. Berne, *Photon Correlation Spectroscopy and Velocimetry* (Ed. by H. Z. Cummins and E.R. Pike, NATO advanced study institutes series: Physics, 1976).
8. D. Magde, E. Elson and W.W. Webb, "Thermodynamic fluctuations in a reacting system-measurement by fluorescence correlation spectroscopy," Phys. Rev. Lett. **29**, 705-708 (1972).
9. R. Rigler, Ü. Mets, J. Widengren and P. Kask, "Fluorescence correlation spectroscopy with high count rate and low background: analysis of translational diffusion," Eur. J. Biophys. **22**, 169-175 (1993).
10. R. Rigler, "Fluorescence correlations, single molecule detection and large number screening. Applications in biotechnology," J. of. Biotechno. **41**, 177-186 (1995).
11. O. Krichevsky and G. Bonnet, "Fluorescence correlation spectroscopy: the technique and its applications," Rep. Prog. Phys. **65**, 251-297 (2002).
12. W. Schrof, J. F. Klinger, S. Rozouvan and D. Horn, "Raman correlation spectroscopy: A method for studying chemical composition and dynamics of disperse systems," Phys. rev. E. **57(3)**, R2523-R2526 (1998).

#189944 - $15.00 USD Received 3 May 2013; revised 13 Jun 2013; accepted 13 Jun 2013; published 20 Jun 2013

13. R. S. Mulliken, "Intensities of electronic transitions in molecular spectra VII. Conjugated polyenes and carotenoids," J. Chem. Phys. **7**, 364-373 (1939).
14. S. F. Parker, S. M. Tavender, N. Mi. Dixon, H. Herman, K. P. J. Williams and W. F. Maddams, "Raman spectrum of beta-carotene using laser lines from green (514.5 nm) to near-infrared (1064 nm): Implications for the characterization of conjugated polyenes," App. Spect. **53**(1), 86-91 (1999).
15. C. Eggeling, J. Schaffer, C. A. M. Seidel, J. Korte, G. Brehm, S. Schneider and W. Schrof, "Homogeneity, transport and signal properties of single Ag particles studied by single-molecule surface-enhanced resonance Raman scattering," J. of Phys. Chem. A **105**(15), 3673-3679 (2001).
16. T. Hellerer, A. Schiller, G. Jung and A. Zumbusch, "Coherent anti-Stokes Raman scattering (CARS) correlation spectroscopy," Chem. Phys. Chem.**7**, 630-633 (2002).
17. J. Cheng, E. O. Potma and S. X. Xie, "Coherent anti-Stokes Raman scattering correlation spectroscopy: Probing dynamical processes with chemical selectivity," J. Phys. Chem. A **106**, 8561-8568 (2002).
18. M. Nishida and E. R. Van Keuren, "Derivation of the optical autocorrelation function from Raman scattering of diffusing particles," J. Mod. Opt. **59**(2), 102-105 (2012).
19. M. Nishida, "Raman correlation spectroscopy: A feasibility study of a new optical correlation technique and development of multi-component nanoparticles using the reprecipitation method," Ph.D. Dissertation, Georgetown University, Washington, D.C., 2011.
20. M. Minsky, "Memoir on inventing the confocal microscope," Scanning **10**, 128138 (1988).
21. R. Webb, "Confocal optical microscopy," Rep. Prog. Phys. **59**, 427-471 (1996).
22. D. W. Schaefer, "Dynamics of number fluctuations: motile macroorganisms," Science **180**, 1293-1295 (1973).
23. S. R. Aragon and R. Pecora, "Fluorescence correlation spectroscopy as a probe for molecular dynamics," J. Chem. Phys. **64**(4), 1791-1803 (1976).
24. N. Thompson, "Topics in fluorescence spectroscopy, Volume I: Techniques," Ed. Joseph R. Lakowicz, Plenum Press, New York (1991).
25. T. J. Herbert and J. D. Acton, "Photon correlation spectroscopy of light scattered from microscopic regions," Appl. Opt. **18**(5), 588-590(1979).
26. A. Barbara, T. López-Ríos, S. Dumont, F. Gay and P. Quémerais, "A microscope spectrometer for light scattering investigations," App. Opt. **49**(22), 4193-4201 (2010).
27. A. Palla-Papavlu, V. Dinca, I. Paraico, A. Moldovan, J. Shaw-steward, C. W. Schneider, E. Kovacs, T. Lippert and M. Dinescu, "Microfabrication of polystyrene microbead arrays by laser induced forward transfer," J. Appl. Phys. **108**, 033111-1-6 (2010).
28. A. Ashkin, "Acceleration and trapping of particles by radiation pressure," Phys. Rev. Lett. **24**(4), 156-159 (1970).
29. A. Ashkin, "Forces of a singe-beam gradient laser trap on a dielectric sphere in the ray optics regime," Biophys. J. **61**(2), 569-582 (1992).
30. A. Ashkin and J. M. Dziedzic, "Optical trapping and manipulation of viruses and bacteria," Science **235**, 1517-1520 (1987).
31. R. Bar-Ziv, A. Meller, T. Tlusty, J. Stavans and S. A. Safran, "Localized dynamic light scattering: Probing single particle dynamics at the nanoscale," Phys. Rev. Lett. **78**(1), 154-157 (1997).
32. N. B. Viana, R. T. S. Freire and O. N. Mesquita, "Dynamic light scattering from an optically trapped microsphere," Phys. Rev. E **65**, 041921-1-11 (2002).
33. C. Hosokawa, H. Yoshikawa and H. Masuhar, "Cluster formation of nanoparticles in an optical trap studied by fluorescence correlation spectroscopy," Phys. Rev. E **72**, 021408-1-7 (2005).
34. M. J. Lang and S. M. Block, "Resource Letter: LBOT-1: Laser-based optical tweezers," Am. J. Phys. **71**, 201-215, (2003).

1. Introduction

Dynamic light scattering (DLS) and Fluorescence Correlation Spectroscopy (FCS) belong to the same widespread class of optical fluctuation spectroscopy experiments by which the thermal fluctuations in colloidal solutions or in reacting systems may be investigated. The origins of these techniques have their roots in the early 20th century with, on the one hand, the work of Gouÿ [1] and that of Einstein [2] who understood the thermal origin of the Brownian motion and thereby the relationship between the diffusion coefficient D of a particle and its size, and the temperature and the viscosity of the solvent. On the other hand we find the studies on the statistics of random walks and stochastic processes [3, 4] which permitted to demonstrate that the thermal noise could be analysed to gain insights in the dynamics of the system. In the field of optical fluctuations, the first experimental achievements resulting from these ideas and knowledge took place in the mid-sixties when the development of the quick electronics and the discovery of the laser enabled to measure the rapid temporal fluctuations of coherent light scat-

#189944 - $15.00 USD Received 3 May 2013; revised 13 Jun 2013; accepted 13 Jun 2013; published 20 Jun 2013

tered by particles in motion [5–7]. Such experiments, known as dynamic light scattering (DLS) or quasi-elastic light scattering, demonstrated the ability of measuring the diffusion coefficient of particles in a dispersion by deriving time-autocorrelation functions of a dynamic variable of the system, here the intensity of the photons elastically scattered by the particles [6]. This intensity being essentially governed by the dielectric constant of the scatterers, it rapidly appeared that this method would not be suited to the study of chemical or biophysical reactions involving different chemical species. Consequently, short after the demonstration of DLS and of its great potential, Madge et al. [8] proposed the FCS technique based on the measure and analysis of the fluctuations of the fluorescence of targeted scatterers and demonstrated the possibility of studying the kinetics of a reaction in a multicomponent system. In 1993, the FCS technique was greatly improved by the introduction of the use of confocal microscopy in the measurements [9]. Thanks to the realization of small observation volumes, the background signal was strongly reduced, the autocorrelation functions of the intensities had a much better signal-to-noise ratio and the sensitivity of the method was enhanced up to the single-molecule detection [10], giving rise to a great number of works and publications [11].

In the original paper of Madge et al. [8], it was already stated that the underlying principle of FCS could be extended to other dynamical variables such as Raman scattering intensities. The great advantage of Raman correlation spectroscopy (RCS) as compared to FCS is that each molecule has its own Raman signature which confers an intrinsic chemical selectivity to the technique. In that sense, RCS is less restrictive than FCS as it is free of labeling and it is not subjected to blinking nor bleaching of the fluorophores. In spite of that only a very few experiments have demonstrated the proof-of-principle of the method. The difficulty in performing RCS measurements is due to the extremely small cross-section of the Raman scattering process. It was only with the development of highly sensitive FCS measurements, and its transposition to RCS, that the first realization of RCS could be achieved by Schrof et al. [12]. Their demonstration was done by illuminating beta-carotene particles with an He-Ne laser, i.e in pre-resonance conditions. Beta-carotene is indeed known to have electronic transitions in the visible range that enhance the Raman cross section of the material [13, 14]. Following this work, a few RCS experiments using different ways of Raman enhancement, namely surface enhanced Raman scattering (SERS) from molecules adsorbed on silver colloid [15] and coherent anti-Stokes Raman scattering (CARS) [16, 17], were performed and also demonstrated the possibility of the method for the investigation of diffusion processes. Nevertheless, in spite of these demonstrations of feasibility done more than ten years ago, RCS was not developed and stagnated in the proof-of-principle state restricted to these cases where amplifications of the Raman signal could be obtained. Recently, however, a group proposed an alternative experimental implementation for RCS measurements [18] aiming at exploiting the coherence of the Raman process. In their case, the experimental set-up is different than the ones used in the previous studies and in FCS. In fact, the apparatus and the underlying principle of their method are based on those of standard DLS measurements, which means that the temporal fluctuations of the Raman intensities are due to the phase shifts of the scattered fields as the scatterers move. The authors derived the optical autocorrelation function of Raman intensities in this configuration [18] and carried out some experiments [19] also on beta-carotene particles illuminated in the visible spectral range.

In the present work we investigated the possibility of performing RCS measurements under a confocal microscope without any amplification of the Raman signal, i.e with much lower Raman cross-sections than in all the previous studies cited here above. For that purpose, we have chosen a model system of aqueous suspension of spherical polystyrene beads of various diameters ranging from 100 to 1000 nm. By comparison with the previous studies [12], the sizes of the particles are equivalent but the Raman cross-section of polystyrene was estimated to be *four orders of magnitude smaller* than that of beta-carotene under an illumination wavelength

#189944 - $15.00 USD Received 3 May 2013; revised 13 Jun 2013; accepted 13 Jun 2013; published 20 Jun 2013

of 514.5 nm [19]. Our experimental set-up has a configuration close to that proposed in the paper of Schrof et al. [12], and the different optical elements were optimize to gain in sensitivity and in signal-to-noise ratio. Obtaining RCS data in full agreement with the one expected from theory demonstrates the possibility of performing quantitative RCS on much weaker Raman scatterers than those of the reported studies.

The paper is organized as follows. In the first section, we describe the optical set-up that was used to perform the RCS measurements. We then give the theoretical expressions of the ACFs used to analyze the experimental results. Next we show the measurements obtained on five solutions containing particles of 100, 200 500 750 and 1000 nm in diameter respectively. The analysis of the data indicates that for particles from 200 to 750 nm in diameter, the ACFs of the Raman intensities enable to determine the diffusion coefficient of the particles accordingly to the theory of free Brownian particles. The case of the largest particles of 1000 nm in diameter is special. We show that in this situation the RCS measurements actually correspond to that of a Brownian particles optically trapped in the confocal volume.

2. Experimental set-up

The experimental set-up is sketched in Fig. 1. The solution is illuminated by an inverted Zeiss microscope equipped with an infinity corrected 100$\times$ oil-immersion objective of numerical aperture 1.45. The illumination is provided by a laser source of wavelength λ_0=532 nm and of power P_0=50 mW at the entrance of the microscope. The backscattered light (Rayleigh and Raman) is collected by the same objective and is focused by a lens tube onto a 300 μm-diameter pinhole placed in the confocal plane. As it is known from confocal microscopy [20, 21] the pinhole is a spatial filter which only allows the photons coming from the focus point to pass through the aperture. Consequently its diameter determines the confocal detection volume. The value of the diameter of the pinhole used here, which is larger than that usually used in confocal microscopy, is very important as its size is such that the observation volume is sufficiently large to measure a Raman signal but not too large to maintain the sensitivity to the fluctuations of the signal. A Notch filter of optical density of 6.0 is placed behind the pinhole to suppress the Rayleigh scattering while the Raman photons are transmitted and focused at the entrance slits of the Raman spectrometer (Spectro Solar TII). In the spectrometer, a 75 grooves/mm grating diffracts the incident beam to disperse spatially the Raman photons of different wavelengths and two types of experiments are possible: (i) the diffracted beam is sent onto a cooled CCD (charge-coupled device) camera (Andor DU 440) to measure the Raman spectra of the sample (Fig. 1(b)), or (ii) the photons of a chosen wavelength are sent onto the exit slits of the spectrometer whose opening is fixed to 0.5 mm. The outgoing beam is collimated onto a 20$\times$ objective which focuses the beam to a spot size of the order of 100 μm in diameter, which is slightly smaller than the diameter of the active area of the avalanche photodiode detector (APD Perkin Elmer, SPCM-AQR-15). Each photon counted exits the APD as a TTL (transistor-transistor logic) pulse which is processed by a photon correlator (Ciprian). The latter measures the time delay between two pulses to reconstruct the intensity I_λ(t) of the Raman photons of the selected wavelength λ as a function of time t. Finally, a software derives the ACF of I_λ(t) (Fig. 1(c)). Let us note that by removing the Notch filter and setting the outgoing wavelength to λ=λ_0=532 nm, DLS measurements can also be performed with our experimental set-up.

3. Autocorrelation functions

The spherical polystyrene beads in suspension in water have a Brownian motion characterized by a diffusion coefficient D from which the diameter of the particles can be derived, accordingly to the Stokes-Einstein formula: $D = k_B T/(3\pi\eta d_H)$, where k_B is the Boltzmann's constant, T

#189944 - $15.00 USD Received 3 May 2013; revised 13 Jun 2013; accepted 13 Jun 2013; published 20 Jun 2013

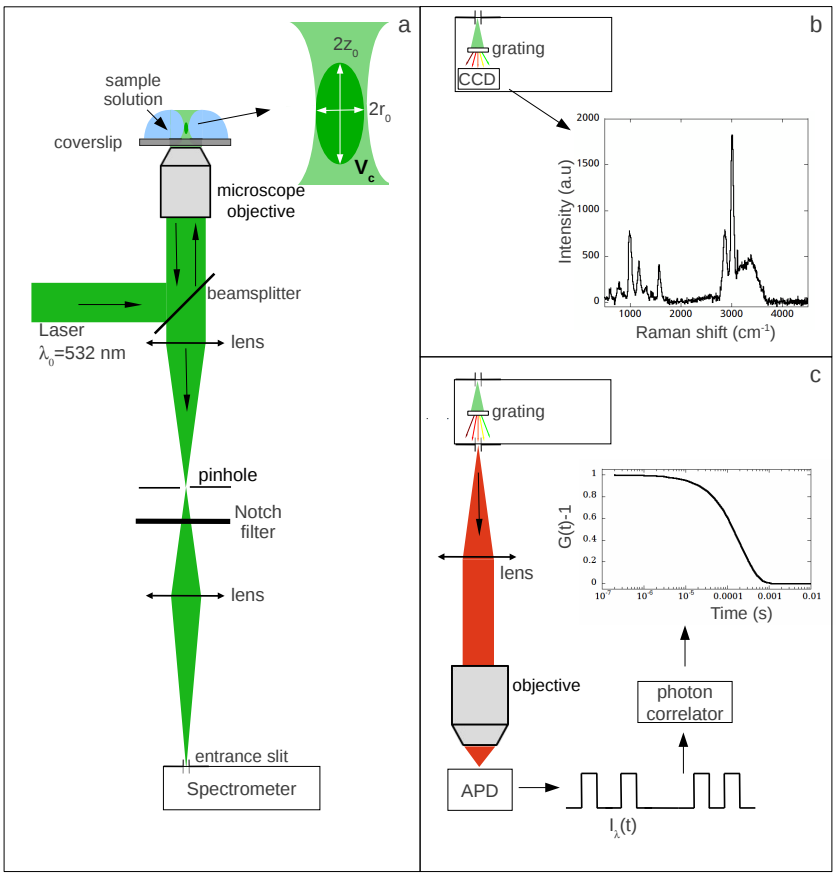

Fig. 1. Scheme of the experimental set-up. (a) The sample is illuminated by a laser of wavelength λ_0=532 nm through a high numerical aperture objective. The back-scattered light is collected by the same objective and is spatially filtered by a pinhole placed in the confocal plane, before being sent to the entrance of the Raman spectrometer. For Raman spectra acquisition and RCS measurements, a Notch filter is placed after the pinhole to ensure the rejection of the elastic light scattering. The light entering the spectrometer is diffracted and the diffracted beam is either (b) sent to a CCD camera for the Raman spectra acquisition or (c) sent through the exit slits whose aperture selects the wavelength λ and the spectral width of the outgoing beam. The latter beam is focused on an APD coupled with a photon correlator which measures the intensity I_λ(t) of the photons of wavelength λ as a function of time. A software calculates the ACF of this intensity.

and η are the temperature and the viscosity of the solvent respectively. d_H is the hydrodynamic diameter of the particle. The measure of D is obtained from the characteristic time of the ACF of the Raman scattering intensities whose fluctuations arise from the variation of the instantaneous number of particles in the confocal volume. The latter volume, in the experimental geometry we use, is generally assumed to have a profile describable by an anisotropic Gaussian function $I(x,y,z) = I_0 e^{-2(x^2+y^2)/r_0^2 - 2z^2/z_0^2}$, where I_0 is the incident intensity, r_0 and z_0 are the radius of the profile in the (x,y) plane and in the z direction respectively, the z direction being parallel to the direction of propagation of the beam (Fig. 1(a)). Accordingly to the theory developed for

#189944 - $15.00 USD Received 3 May 2013; revised 13 Jun 2013; accepted 13 Jun 2013; published 20 Jun 2013

DLS [22] and FCS [23] experiments in such small volumes, the ACF writes as:

$$G(t) = \frac{\langle I(\tau)I(\tau+t)\rangle}{\langle I(\tau)\rangle^2} = 1 + \frac{c^2}{\langle N\rangle}\frac{1}{(1+t/\tau_D)\,(1+t/(w^2\tau_D))^{0.5}}, \quad (1)$$

where $\tau_D = r_0^2/4D$ is the characteristic time of the translational diffusion and $w = z_0/r_0$ is the shape parameter of the confocal volume. $\langle N\rangle$ is the average number of scatterers in the confocal volume and $c = 1 - I/I_B$ is the background correction factor, I being the total intensity and I_B that of the background [24]. The expression Eq. (1) will be used in the next paragraph to analyze the experimental results obtained for the Brownian particles.

It is also well known that when the scattered light is coherent there is another source of thermal fluctuations. In that case, the measured intensity indeed results from the interferences of all the electric fields scattered by the different particles in the observation volume. The phases of these fields depend on the relative position of the scattering centers, and consequently, the value of the resulting intensity changes with the motion of the particles. These intensity fluctuations give birth to an ACF of the form:

$$G_c(t) = 1 + \beta e^{-2q^2Dt}, \quad (2)$$

where $\vec{q}$ is the scattering vector defined as $\vec{q} = |\vec{k}_s - \vec{k}_i|$ where $\vec{k}_s$ and $\vec{k}_i$ are the wave vectors of the scattered and incident waves respectively and $0 < \beta < 1$ is the intercept value $G_c(0) - 1$, related to the number of coherence areas seen by the detector [7].

When the experiments are conducted with a high numerical aperture objective, many different values of the scattering vector co-exist and the angle of collection is larger than the angle of coherence [25], both effects leading to a large decrease of β. As a result, this additional contribution is not (for RCS), or only very weakly (for DLS), measured in our experimental configuration and the ACFs essentially behave as described by Eq. (1) [26]. In contrast, in the experimental set-up proposed in [18], the ACFs are of the form of Eq.(2).

4. Experimental results for free Brownian particles

Before performing the RCS measurements, the temperature of the solvent and the size of the confocal volume were calibrated by measuring the DLS and FCS ACFs on commercial solutions containing red fluorescent carboxylate-modified polystyrene (PS) beads (Sigma-Aldrich) of known diameters. We found a temperature of $T = 24°C$ and a confocal volume of radius $r_0 = 450 \pm 50$ nm and of shape factor w^2=10.

The RCS measurements were performed on commercial (Polysciences) Polybead PS micro spheres in a 2.5 wt.% aqueous suspension with 100, 200, 500, 750 and 1000 nm in nominal diameter. In the following we will consider that the particles are large enough to assimilate the hydrodynamic diameter (d_H) to the nominal one (d_N) and both of these diameters will be denoted as d. Raman spectra of the solutions were recorded during 30 s and present the expected Raman bands of PS [27] and the large water band around 3400 cm^{-1}, as can be seen on Fig. 1(b). RCS measurements were done by deriving the ACF of the intensity of the most intense Raman band namely the one at 3005 cm^{-1} corresponding to the aromatic CH stretch of the PS [27]. Measurements typically last 10 s and and reproduced 10 times to lower the noise signal in the ACFs.

4.1. Particles of nominal diameter d=100 nm

Raman spectra recorded on this solution show very weak PS Raman bands of only a few tens of counts per second. Unsurprisingly, the measured ACFs were very flat and noisy indicating that

#189944 - $15.00 USD Received 3 May 2013; revised 13 Jun 2013; accepted 13 Jun 2013; published 20 Jun 2013

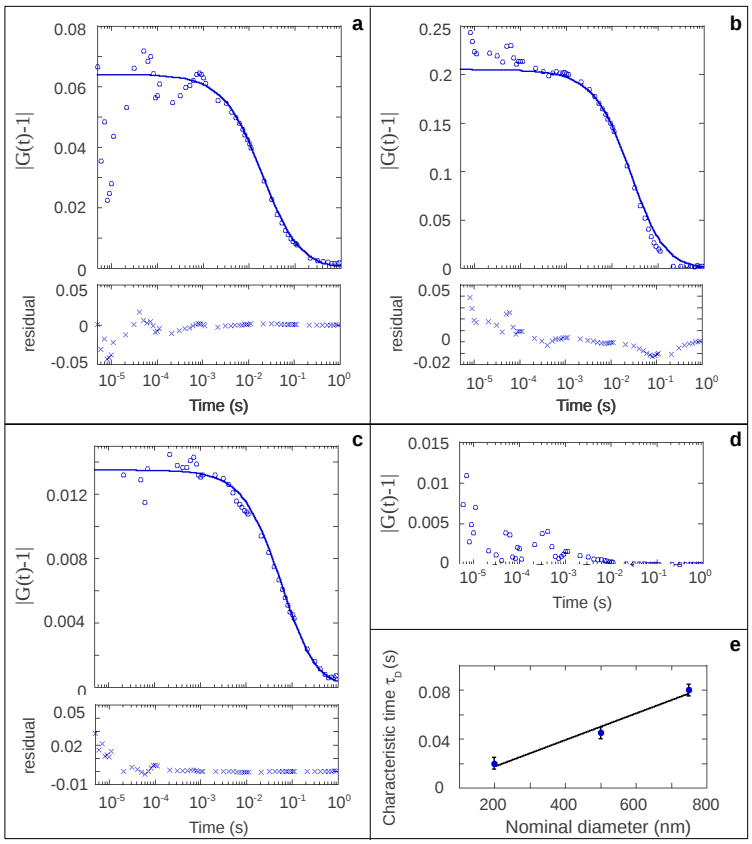

Fig. 2. (a-c) ACFs of the Raman intensities located at 3005 cm^{-1} scattered by PS particles of different sizes: d=200 nm (a), d=500 nm (b) and d=750 nm (c). (d) ACF of the Raman intensity scattered by the water molecules and located at 3400 cm^{-1}. Dots are the experimental data and full lines the calculated ones using Eq. (1). The characteristic times of the ACFs are τ_D=20 ms for d=200 nm (a), τ_D=45 ms for d=500 nm and τ_D=80 ms for d=750 nm. (e) Plot of the characteristic times as a function of the diameter of the particle. The error bars come from the different values obtained from measurements on the same bead sizes. The slope of the line expresses as $a = 3\pi\eta r_0^2/(4k_BT) = 1.036 \times 10^{-4}$ s.nm^{-1} and gives access to the radius of the confocal volume $r_0 = 445 \pm 50$ nm at $T = 24°C$.

no correlation curves could be derived from the fluctuations of the Raman intensity. In order to check the quality of the solution, DLS experiments were performed in the experimental configuration described above (output wavelength of the spectrometer λ=532 nm and removal of the Notch filter). We measured an ACF with a temporal decay and a characteristic time corresponding to the one expected for 100 nm-diameter diffusive particles. Consequently, the absence of RCS ACFs cannot be attributed to the quality of the sample but is due to the fact that the Raman signal of an individual particle is too small as compared to the background signal.

4.2. Particles of nominal diameter d=200, 500 and 750 nm

The ACFs derived from the Raman band at 3005 cm^{-1} are shown in Figs. 2(a)-2(c), together with the ACF derived from the Raman intensity of water (Fig. 2(d)). One clearly sees the presence of a temporal decay on the ACFs measured on the PS Raman band whereas a flat

#189944 - $15.00 USD Received 3 May 2013; revised 13 Jun 2013; accepted 13 Jun 2013; published 20 Jun 2013

and noisy ACF is obtained from the Raman of water even though its mean intensity is larger than that of the PS particles. This is due to the fact that the water molecules are small and thus numerous in the observation volume so that the intensity which scales as $< N >$ is large but the fluctuations which scale as $1/ < N >$ tend to 0 (Eq. (1)). Moreover, the ACFs of the PS beads, represented by dots in Fig. 2, are properly reproduced by the ACFs calculated (full line) with Eq. (1), which indicates that the observed temporal behavior is correct and behaves as $G(t) \sim t^{-3/2}$ as is expected for Brownian particles. In the experimental ACFs, the noise at short times comes from the photon correlator. For the short sampling times the random noise is indeed higher that for larger sampling times and, moreover, there is a sharp effect of the statistical fluctuations since only a very few Raman photons are counted due to the weak Raman intensities. Let us note that this later contribution to the short time delay noise diminishes when increasing the signal as can be seen in Fig. 3. The calculated ACFs are fitted to the experimental ones by adjusting the characteristic time τ_D and the intercept value $G(0) - 1$. For the 200 nm-diameter beads, a shape factor w^2=10 was found to reproduce the ACF correctly whereas a value of w^2=1 suits better the ACFs obtained from the solutions with larger particles. This is due to the fact that the ACFs have a steeper time-decay when the size of the particles becomes comparable with the waist of the confocal beam. This effect has been reported several times in the literature [12, 16]. A good agreement between the calculated ACFs and the experimental ones are found for $\tau_D = 22.5\pm$ 2.5 ms, 45$\pm$ 5 ms and 80$\pm$ 5 ms for the solutions containing particles of diameter d=200, 500 and 750 nm respectively. The error bars come from the different characteristic time measured on the same bead sizes. Fig. 2(e) shows the plot $\tau_D = f(d)$ of the values of the characteristic times τ_D as a function of the diameters of the particles for which a linear behavior is expected as $\tau_D = r_0^2 \times 3\pi\eta d_H/(4k_BT)$. A line is indeed observed in Fig. 2(e) and this is an additional confirmation of the validity of our RCS measurements. Moreover, the radius of the confocal volume can be accessed since it derives from the slope of the line. The value found for the latter slope is $a = 1.036 \times 10^5$ s.m^{-1}. Its value yields $r_0 = 445\pm$ 50 nm considering the temperature of the solvent $T = 24°C$ and the tabulated value of its viscosity at this temperature $\eta_{24°C} = 0.911 \times 10^{-3}$ kg.m^{-1}s^{-1}. This value of r_0 is in full accordance with the one already estimated from FCS measurements.

In principle, the ACFs also permit to access the mean number of particles in the confocal volume (Eq. (1)) from the intercept value $G(t = 0) - 1$. However this requires either to have a high signal to background ratio (c tends to 1) or to be able to determine the value of the background signal precisely. In the study presented here, the Raman band of the PS from which the ACFs are derived is partially convoluted with the Raman band of water which is a source of background. Moreover, the nominal concentration of the solutions, with particles of size $d >$200 nm, are such that $< N >_{nominal}$ is smaller than 1. Therefore, during a part of the measuring time, only the background signal coming from the Raman scattered by the molecules of water is measured. The value of c is thus small and difficult to estimate and no determination of $< N >$ was possible here. Further studies will be made to be able to access this parameter. A way to do it is to estimate the Raman background signal by measuring time integrated intensities at different wavelengths scanned through the Raman band of interest.

5. Experimental results for an optically trapped particle

In the case of the larger particles of nominal diameter d=1000 nm, RCS measurements are easier to realize. This increased sensitivity of the experiment obviously comes from the size of the particle which, on the one hand, contains many molecules responsible for a high Raman signal, and, on the other hand, induces strong fluctuations when passing the confocal volume. Consequently, ACFs were successfully obtained on the five observed Raman bands of the PS whereas only the most intense band located at 3005 cm^{-1} led to measurable ACFs for the

#189944 - $15.00 USD Received 3 May 2013; revised 13 Jun 2013; accepted 13 Jun 2013; published 20 Jun 2013

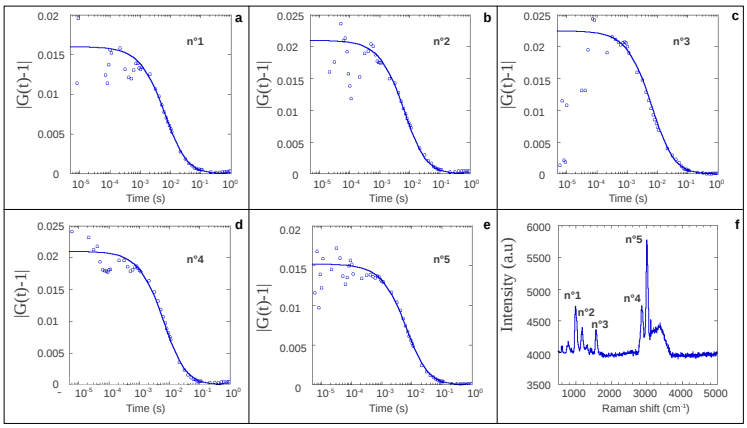

Fig. 3. (a-e) ACFs of the Raman intensity scattered by PS particles of size d=1000 nm and located at 990 cm^{-1} (a), 1175 cm^{-1} (b), 1570 cm^{-1} (c), 2865 cm^{-1} (d) and 3005 cm^{-1} (e) 3005 cm^{-1}. Dots are the experimental data and full lines the calculated ones using Eq. (1). The characteristic time is the same for all the measurements and equals $\tau_D = 10$ ms. (f) Raman spectra of the solution integrated over 30 s.

smaller particles. Fig. 3 shows the five ACFs derived from the different Raman bands of the PS particles, together with the Raman spectra of the solution. The dots are the experimental points and the lines are the calculated ones using Eq. (1). A good agreement can be found between the experimental curves and the calculated ones when considering w^2=1 and for τ_D=10 ms. This characteristic time is however one order of magnitude smaller than the one expected for a diffusive motion of the particles. Yet, all the ACFs present the same time-decay behavior and this reproducibility is a strong indication of the validity of the measures.

An explanation to this result is that we measured the ACFs of a single particle *trapped* in the confocal volume. We know for a fact from the work of Ashkin et al. [28] that forces of radiation pressure of a continuous laser permit to suspend micro-sized dielectric particles and that a highly focused single-beam laser (as we have in our experiment) is very efficient to produce such an optical trap [29, 30]. To check the validity of this hypothesis we answered two questions: (i) are the derived ACFs measured in RCS experiments compatible with the ACF expected for a trapped particle? and (ii) does reducing the incident power of the laser release the bead?

The temporal fluctuations of the scattered intensity related to the Brownian motion of a trapped particle was first studied by Bar-Ziv et al. [31] and later by Viana et al. [32]. In their work, a micro-sized dielectric particle is trapped by a laser focused by a high numerical aperture objective and DLS experiments are performed with a second probe laser. The latter, of different wavelength, is focused by the same objective and has a power sufficiently small to consider that it does not play any role in the trapping of the particle. Our experimental set-up is very analogous to this arrangement, the trapping being performed by the incident laser and the probe of the temporal fluctuations being the Raman photons. FCS in such a configuration have also been reported [33]. In DLS, FCS or RCS from an optically trapped particle, the time-fluctuation of the intensity is due to the motion of the particle within the non-uniform intensity profile of the focus spot. In the weak trapping regime, the optical forces only slightly affect the Brownian motion of the particle which will be slowed down in the focus spot but keeps the ability of escaping it. As a consequence, ACFs still present a time-decay of the form $G(t) \sim t^{-3/2}$ with a characteristic time larger than the one measured for a non-trapped Brownian particle, repre-

#189944 - $15.00 USD Received 3 May 2013; revised 13 Jun 2013; accepted 13 Jun 2013; published 20 Jun 2013

sentative of the increase of the transit time of the particle through the focal spot. This is not what we observed. In the strong trapping limit, the motion of the particle is that of a Brownian particle in a potential well. The latter is approximatively harmonic with a restoring force $-k_i r_i$, with $i = x, y, z$, acting on the particle. It has been shown that in this case, and assuming that $k_x = k_y$, the ACF takes the form [31, 32]:

$$G(t) = 1 + A_x e^{-t/\tau_x} + A_z e^{-t/\tau_z}, \tag{3}$$

where $\tau_x = 3\pi\eta d/k_x$ and $\tau_z = 3\pi\eta d/k_z$ are the characteristic times of the motion of the particle in the transverse plane and in the longitudinal direction respectively. They are related to the stiffness of the trap k_x and k_z in the direction x and z respectively. A_x and A_z are the amplitudes related to the waist of the laser beam and the stiffness of the trap. In this regime the time-decay becomes exponential-like and the characteristic times are smaller than those observed in the free particle case.

To verify if this case can explain the observed ACFs, our RCS experiments were fitted with the Eq. (3). The resulting ACF is shown in Fig. 4(a) (light blue line) together with the ACF measured from the Raman band located at 3005 cm^{-1} (light blue dots). The two exponentials of Eq. (3) are represented in dotted light blue lines. To highlight the change of behaviour of the measured ACF as compared to the case of a freely diffusive particle of the same size, we also calculated the ACF expected in the free Brownian situation, using the Eq. (1) and plotted it in a dark blue line. From Fig. 4(a), one can see that a good agreement between the measure and the calculation can be found, indicating that the exponential-like decay suits the experiments. In order to see better the difference between the exponential-like and the power law time decay of the trapped and the free particle respectively, the same data as that of Fig. 4(a) are plotted in a y-axis logarithmic scale in Fig. 4(c). The fitting parameters obtained from adjusting the experiments to Eq. (3) are $\tau_x \sim$7 ms and $\tau_z \sim 6\tau_x$ for the characteristic times and $A_x \sim$0.01 and $A_z \sim$0.003 for the amplitudes. They are in full agreement with the ones found in the literature [31, 32] that give typical values for $\tau_x \sim$5-20 ms depending on the intensity of the beam and the diameter of the particles, and an optical trap anisotropy $\tau_z \sim 6 - 10\tau_x$ and $G(0) - 1 \sim$0.02. Our RCS measurements are thus compatible with the theoretical model of a Brownian particle in a harmonic potential.

We also verified the effect of the power of the incident laser on the motion of the particle. This cannot be done while performing RCS measurements as the Raman signal becomes too small if the incident (excitation) intensity is reduced. Therefore, we realized DLS experiments (i) in the same experimental conditions than the RCS ones i.e with a high power illumination and (ii) with an incident power reduced by four orders of magnitude by a density filter. We expected to trap the particle in the former case and not in the second one. The ACFs measured in both of these configurations are presented in Fig. 4(b) with a linear y-axis scale and in Fig. 4(d) with a logarithmic y-axis scale. A clear change of behaviour is observed between the two cases: for a strong illumination, the ACF presents an exponential-like decay with a characteristic time $\tau_x \sim$6.5 ms. The DLS ACF is thus very similar to the RCS one despite the fact that the second exponential expected from Eq. (3) is not measured in DLS. This could be due to the fact that we used the same laser to trap the particle and to probe its motion. When the illumination power is reduced, the ACF presents a much larger characteristic time $\tau_x \sim$100 ms and its time decay obeys the power law $G(t) \sim t^{-3/2}$. Both of these features are the ones expected for a freely diffusive particle. The influence of the incident laser intensity on the motion of the particle is thus clearly established and confirms the hypothesis of localized RCS measurements from a single particle trapped in the confocal volume.

#189944 - $15.00 USD Received 3 May 2013; revised 13 Jun 2013; accepted 13 Jun 2013; published 20 Jun 2013

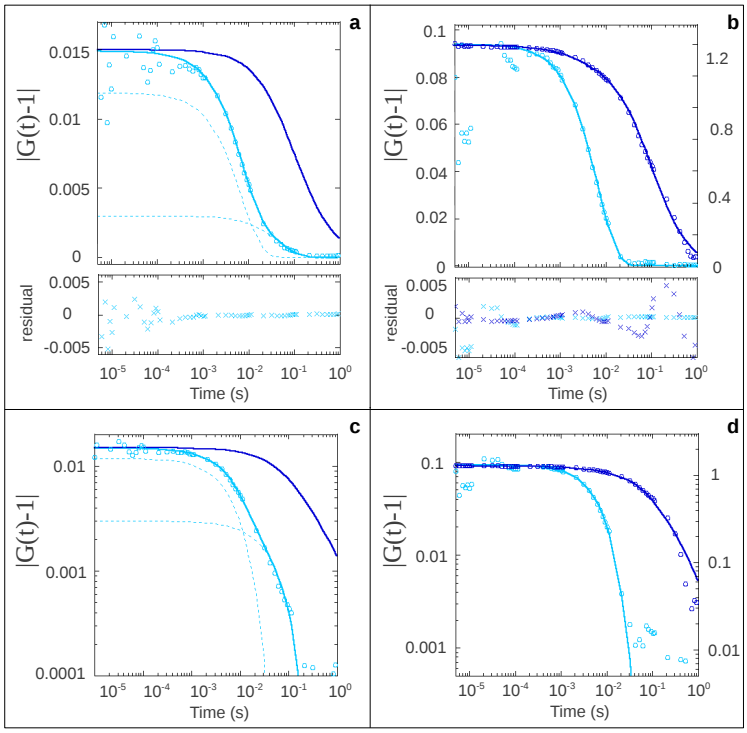

Fig. 4. (a) Experimental ACF (light blue dots) derived from the Raman intensity scattered by a PS particle of size d=1000 nm and located at 3005 cm^{-1}. The theoretical ACF (light blue line) is calculated within the model of a trapped single-particle, using Eq. (3) composed of the sum of two exponentials represented by the two dotted light blue lines. Their characteristic times are τ_x=7 ms and $\tau_z = 6\tau_x$ and their amplitudes are A_x =0.01 and A_z =0.003. The ACF expected for the same particle but animated by a free Brownian motion is shown in dark blue line for comparison. (b) Experimental ACF derived from the elastic scattering from PS particles of size d=1000 nm, at strong (light blue dots) and low (dark blue dots) incident power of the laser. The experiments are in agreement with the model of a trapped single-particle (light blue line) in the case of the strong power illumination and with that of a free Brownian particle (dark blue line) in the case of the low power illumination with respective characteristic times of τ_x=7 ms and τ_D=100 ms. (c) and (d) Same plot as (a) and (b) respectively with a logarithmic y-axis scale to highlight the different time-decay laws of the ACFs in the trapped and free particle configurations.

6. Conclusion

We have presented RCS measurements performed on polystyrene spheres in suspension in an aqueous solution. Different diameters of particles were studied and successful ACFs were obtained for particles of diameter greater than or equal to 200 nm. These results, in terms of sizes of the object studied, are comparable to those claimed in the papers of proof-of-principle of the method. However, in the present study, no amplification of the Raman signal is present, and, in spite of a Raman cross-section several orders of magnitude smaller than that of the beta-carotene particles previously studied [12], correct values of the characteristic times could be obtained. It was also shown that in the case of the 1000 nm-diameter particle, the measured ACFs correspond to that of a single-particle trapped in the confocal volume. To our knowledge, this is the first report of localized RCS experiments.

#189944 - $15.00 USD Received 3 May 2013; revised 13 Jun 2013; accepted 13 Jun 2013; published 20 Jun 2013

The study that we have undertaken still needs further investigations and methodology developments. For instance, it needs a more correct quantification of the local concentration or of the stiffness of the trap in the case of localized RCS. The study of localized RCS on smaller particles was also not done in the present paper. It is however possible to trap dielectric beads of diameters of a few hundreds of nanometer [31] on which RCS could also be realized. Localized RCS could find applications in studying the mechanical properties of biological objects [34] or in growth/aggregation processes of trapped particles [33]. Other chemical bonds are also to be studied in order to have a wider view of the possibilities offered by RCS. We however think that the results presented here are already of interest as they show the possibility of performing RCS measurements on sub-micrometric objects without any amplification of the Raman signal. This makes the technique applicable without any invasive manipulation of the sample and could be very useful in the dynamic characterization of specific component in complex systems.

Acknowledgments

We wish to thank the Région Rhône Alpes for support of this research via the grant CIBLE-RCS. The authors are also indebted to T. López-Ríos and A. Ibanez for many interesting and stimulating discussions and to René Kullock for discussions and help in the lab.

#189944 - $15.00 USD Received 3 May 2013; revised 13 Jun 2013; accepted 13 Jun 2013; published 20 Jun 2013